*Int. J. Solids Structures* Vol. 28, No. 7, pp. 859–877, 1991
Printed in Great Britain.

0020-7683/91 $3.00 + .00


# EFFECT OF BOUNDARIES AND INTERFACES ON SHEAR-BAND LOCALIZATION

A. NEEDLEMAN and M. ORTIZ
Brown University, Division of Engineering, Providence, RI 02912, U.S.A.

(*Received* 14 *September* 1990; *in revised form* 17 *January* 1991)

**Abstract**—The emergence of general stationary-wave solutions, exemplified by Rayleigh surface waves and Stoneley interface waves, is taken as a criterion for the onset of localization in the presence of geometrical features such as free boundaries and interfaces. The stationary-wave solutions yield the possible orientations of the emerging shear bands. The influence of interfaces in crystalline solids and of free boundaries in pressure-sensitive frictional materials is investigated within this general framework. It is found that grain boundaries in polycrystals can act as both barriers to, and as sources of, shear bands. The analysis of pressure-sensitive frictional materials reveals a mismatch in orientation between the shear bands in the interior and on the boundary of the solid. The implications of this misorientation for the global behavior of specimens tested in plane strain compression are discussed.

## 1. INTRODUCTION

While it is clear that interfaces and free surfaces play an important role in the development of localized deformation patterns, the nature of that role depends on specific circumstances. For example, the mismatch in mechanical properties at an interface can induce stress and strain concentrations that act as initiation sites for localization. Conversely, internal interfaces, e.g. grain boundaries, can act as barriers to localizations that originate in bulk material. The orientation of localized deformation bands is often observed, both in experiment and in numerical simulations, to change when free boundaries are approached. The effect of this orientation change on the overall response remains to be clarified.

Here, attention is restricted to time- and rate-independent materials and localization is associated with vanishing wave speeds. The correspondence between stationary body waves and bulk localization has long been appreciated (Hadamard, 1903; Hill, 1962; Biot, 1963a; Mandel, 1966; Rice, 1977). More recently, the broader connection between stationary waves, stability and well-posedness of boundary value problems has received considerable attention (Simpson and Spector, 1987, 1989; Dowaikh and Ogden, 1990). What is perhaps not so widely appreciated is that a variety of stationary waves can be interpreted in terms of bands of localized deformation. When viewed this way, results on stationary Rayleigh waves (free surface waves) and on stationary Stoneley waves (interface waves) give a perspective on the interaction between shear bands, free surfaces and interfaces. A characteristic direction is associated with each type of stationary wave and this characteristic direction defines the orientation of the localization.

We present a formulation of stationary body, Rayleigh and Stoneley waves that stresses the relation to localization and that emphasizes the uniformity of the analysis for each type of wave. The circumstances considered are such that no characteristic geometric length enters the problem formulation. Hence, the wavelength of the stationary waves is undetermined. Since this wavelength can then be arbitrarily short, the critical condition for stationary waves can be regarded as a local criterion. Specific results are given for two cases. In one case, a plane strain crystal model is used to explore, within the stationary wave framework, the role of crystal misorientation across grain boundaries in precipitating shear-band development or in acting as a barrier to shear-band propagation. In the other case, shear-band orientation changes at free surfaces are analyzed for pressure-sensitive dilational solids. The possible large effect of these orientation changes on the overall response is discussed.

## 2. GOVERNING EQUATIONS

We consider deformations that take the material point initially at $\mathbf{x}$ to $\bar{\mathbf{x}}$, where both $\mathbf{x}$ and $\bar{\mathbf{x}}$ are referred to a fixed Cartesian frame. The displacement vector $\mathbf{u}$ and the deformation gradient $\mathbf{F}$ are defined by

$$\mathbf{u} = \bar{\mathbf{x}} - \mathbf{x} \quad \mathbf{F} = \frac{\partial \bar{\mathbf{x}}}{\partial \mathbf{x}}. \tag{1}$$

In terms of the unsymmetric nominal stress tensor, $\mathbf{t}$, which is related to the traction, $\mathbf{T}$, transmitted across a material element of area having orientation $\boldsymbol{\nu}$ in the reference configuration by $\mathbf{T} = \boldsymbol{\nu} \cdot \mathbf{t}$, balance of linear momentum requires

$$t_{ij,i} = \rho \frac{\partial^2 u_j}{\partial t^2} \tag{2}$$

where $\rho$ is the mass density of the body in the reference configuration and $(\ )_{,i}$ denotes partial differentiation with respect to $x_i$. Writing (2) in rate form gives

$$\dot{t}_{ij,i} = \rho \frac{\partial^2 v_j}{\partial t^2} \tag{3}$$

where $(\dot{\ })$ denotes differentiation with respect to time and $v_i = \dot{u}_i$. Similarly, traction-free boundary conditions can be expressed in rate form as

$$\nu_i \dot{t}_{ij} = 0. \tag{4}$$

Throughout subsequent discussions, the material is modelled as rate independent and the constitutive relation is expressed as

$$\dot{t}_{ij} = K_{ijkl} \dot{F}_{lk} = K_{ijkl} v_{l,k}. \tag{5}$$

For elastic–plastic solids exhibiting piecewise-linear behavior, the neighborhood of the current state in strain rate space can be divided into a number of cones, in each of which a linear relationship between stress rate and strain rate holds. For example, the constitutive relation for the classical elastic–plastic solid is piecewise linear with two branches; one for plastic loading and the other for elastic unloading. However, here attention is confined to incrementally-linear solids for which the tensor of moduli $\mathbf{K}$ is fixed by the current state. The specific constitutive equations considered are expressed as a relation between some objective rate of the symmetric Cauchy stress, $\boldsymbol{\sigma}$, or Kirchhoff stress, $\boldsymbol{\tau}$, and the rate of deformation tensor, $\mathbf{d}$. The Cauchy and Kirchhoff stresses are related to $\mathbf{t}$ through

$$t_{ij} = F^{-1}_{ik} \tau_{kl} = J F^{-1}_{ik} \sigma_{kj} \tag{6}$$

where $J = \det(\mathbf{F})$ is the ratio of the volume of a material element in the current configuration to its volume in the reference configuration, $(\ )^{-1}$ denotes the inverse, the Cartesian components of $\mathbf{d}$ are given by

$$d_{ij} = \tfrac{1}{2}(l_{ij} + l_{ji}) \tag{7}$$

and

$$l_{ij} = \dot{F}_{ik} F^{-1}_{kj} \tag{8}$$

are the spatial velocity gradients.

For an incompressible solid, the constraint

$$l_{kk} = v_{k,k} = 0 \tag{9}$$

must be satisfied. The hydrostatic stress then enters the formulation as a Lagrange multiplier and the constitutive relation only specifies the deviatoric response. Accordingly, (5) and (3) become, respectively,

$$\dot{t}_{ij} = K_{ijkl} v_{l,k} + \dot{p}\delta_{ij} \tag{10}$$

and

$$\dot{t}_{ij,i} + \dot{p}_{,i} = \rho \frac{\partial^2 v_j}{\partial t^2}. \tag{11}$$

Constitutive relations for plastic solids are most conveniently expressed in terms of a relation between an objective rate of Cauchy or Kirchhoff stress and the rate of deformation tensor. Standard kinematic identities can then be used to express the constitutive relation in the form (5) or (10). For example, if **L** denotes the moduli relating the convected (also known as the Oldroyd or Lie) derivative of Kirchhoff stress to **d**, then, with the current configuration as reference, the Cartesian components of **K** and **L** are related by

$$K_{ijkl} = L_{ijlk} + \tau_{ik}\delta_{jl}. \tag{12}$$

## 3. STATIONARY WAVES AND LOCALIZATION

Consider a homogeneous solid subject to boundary conditions that are consistent with continuing homogeneous deformations. The response to small wave disturbances about this state can be investigated for an incrementally-linear solid having moduli corresponding to the active moduli for continued homogeneous deformation. For elastic–plastic solids for which $K_{ijkl} = K_{klij}$ this is the linear comparison solid of Hill (1958). For solids lacking this symmetry, the linear comparison solid provides an upper bound (Raniecki and Bruhns, 1981). For piecewise-linear elastic–plastic behavior and with the current state involving "total loading", in the sense that each plastic branch, once activated, remains active, the moduli of the linear comparison solid are those for continued total loading.

For wave solutions superposed on some current state, the relation between a solution for an incrementally-linear solid and the corresponding solution for the underlying elastic–plastic solid is problematical. We presume that the behavior of the linear comparison solid reflects that of the underlying elastic–plastic solid, but the connection is not pursued here. However, it should be noted that at least for solids with this symmetry of the tangent moduli, the critical condition for a vanishing wave speed corresponds to the critical condition for bifurcation.

As is well known, the existence of stationary body wave disturbances, signals the onset of bulk localization (Hadamard, 1903; Hill, 1962; Biot, 1963a; Mandel, 1966; Rice, 1977). The aim here is to explore the effects of boundaries and interfaces on localization by considering conditions for stationary waves where boundary conditions do play a role. In particular, we consider stationary Rayleigh waves along stress-free boundaries and stationary Stoneley waves along interfaces. The significance of stationary waves stems from their role in signifying the transition from stability to instability; when all possible wave speeds $c$ are such that $c^2 > 0$, then there is stability with respect to small disturbances; when $c^2 < 0$ for some waves, there is divergence type growth, as discussed by Rice (1977). In addition, when the incremental moduli fail to be symmetric, the governing equations can admit complex solutions for $c^2$ that correspond to flutter-type instabilities.

Several connections between the stationary-wave characterization of material instability and other alternative theories are noteworthy. Localization in the rate-independent solid can be thought of as a local bifurcation whereby two incremental solutions become possible: one having continuous deformation gradients; the other exhibiting a discontinuity

in the deformation gradients. Discontinuities in the deformation gradients can only occur along characteristic directions. Therefore, the onset of localization coincides with the loss of ellipticity of the incremental equations. Consequently, the boundary value problem becomes ill-posed following localization.

A problem may become ill-posed, however, while the incremental field equations remain elliptic, as a consequence of the failure of the complementing condition at the boundary. Thompson (1969) and Benallal *et al.* (1989) have noted that the failure of the complementing condition is equivalent to the existence of stationary Rayleigh surface waves. An analogous condition for an ill-posed problem that arises in cases where interfaces are present is the existence of stationary Stoneley waves. Similar to the localization condition, the stationary Rayleigh and Stoneley wave conditions determine the orientation of shear bands intersecting free surfaces and interfaces, respectively. In cases where the equations remain elliptic, the stationary wave analysis determines the length of decay of the surface and interfacial modes. Our stationary wave analyses are related to the surface instabilities investigated by Biot (1963b) and Hutchinson and Tvergaard (1980), to the short wavelength limit of the bifurcation solution obtained by Hill and Hutchinson (1975) for plane strain, by Triantafyllidis (1980) in pure bending for solids obeying normality and by Needleman (1979) for plane strain and for solids where the symmetry $K_{ijkl} = K_{klij}$ is lacking, and to the interface instabilities analyzed by Biot (1963c).

Depending on boundary conditions and material constitutive behavior, long-wavelength diffuse modes can become available for finite bodies prior to the onset of localization. In such situations, the stationary wave analysis may, as noted above, correspond to a short-wavelength limit. However, the short-wavelength limit of finite specimen bifurcations and the local stationary wave analysis may yield different results. A notable example is the short-wavelength limit of the diffuse bifurcation solutions of Needleman (1979) in the hyperbolic regime. From these solutions it is concluded that bifurcation into a sufficiently-short wavelength mode is possible as soon as the hyperbolic regime is entered, that is immediately after localization in the bulk. By contrast, our local stationary wave analysis predicts that localization in the bulk may precede localization at the surface by a finite amount in frictional solids. A closer inspection, however, reveals that the two analyses need not be equivalent. Thus, the diffuse bifurcation solutions of Needleman (1979) combine modes emanating from both sides of the specimen, whereas our local analysis considers modes about one surface only, i.e. corresponds to a semi-infinite solid. Furthermore, in the hyperbolic regime the short-wavelength limit does not reduce to the semi-infinite solid case, since the two surfaces of the solid, no matter how distant, always interact. Because the solution space in the diffuse bifurcation analysis is larger than that for the local analysis, the former necessarily predicts critical conditions for localization which precede the local conditions.

*Body waves*

The wave solutions are written in the form

$$v_j = A_j \exp\left[\mathrm{i}(k_k x_k - \kappa c t)\right] \tag{13}$$

where $\mathrm{i} = \sqrt{-1}$, $\kappa = |\mathbf{k}|$, and the components of $\mathbf{k}$ can be complex. Substituting (13) into (3) and using (5) with incremental linearity gives

$$A_i k_k k_l K_{ijkl} = -\rho \kappa^2 c^2 A_j \tag{14}$$

after canceling the common factor $\exp\left[\mathrm{i}(k_k x_k - \kappa c t)\right]$. For stationary waves, $c \equiv 0$, (14) becomes

$$A_i k_k k_l K_{ijkl} = M_{ji} A_i = 0 \tag{15}$$

which admits a non-trivial solution when

$$\det(\mathbf{M}) = 0. \tag{16}$$

Writing $\mathbf{k} = \kappa\mathbf{n}$, real solutions to (15) and (16) give the condition for localization with characteristic directions defined by $\mathbf{n}$, which is the band normal. For a given deformation history, the orientation $\mathbf{n}$ giving the earliest localization is of primary interest. Since no boundary conditions are imposed, the stationary waves obtained from (15) and (16) pertain to an infinite solid.

*Rayleigh waves*

Let the solid extend over the half-space $x_1 \geqslant 0$, and be free of tractions on the boundary $x_1 = 0$. Consider Rayleigh wave solutions of the type

$$v_j = A_j \exp[\mathrm{i}(k_k x_k - \kappa c t)] \tag{17}$$

where, now, $\kappa^2 = k_2^2 + k_3^2$. For these solutions to decay exponentially into the body, the condition

$$\mathscr{I}m\, k_1 \geqslant 0 \tag{18}$$

needs to be satisfied. Inserting (17) into (3) we obtain (14).

We now look for stationary-wave solutions with $c = 0$. Under these conditions, (14) reduces to (15), which has non-trivial solutions if (16) is satisfied. Note, however, that $k_1$ may now be complex, due to the one-sided character of the solution. Assume that for fixed $\kappa$ there are three complex solutions of (14), say $k_1^{(\alpha)}$, $\alpha = 1, 2, 3$, lying on the right-half complex plane. Let $A_j^{(\alpha)}$, $\alpha = 1, 2, 3$, be the corresponding amplitudes. Thus, the general form of the solution is

$$v_j = \sum_{\alpha=1}^{3} A_j^{(\alpha)} \exp[\mathrm{i}(k_k^{(\alpha)} x_k - \kappa^{(\alpha)} c t)]. \tag{19}$$

Furthermore, the amplitudes $A_j^{(\alpha)}$ must be compatible with (15). Thus, if $q_l^{(\alpha)}$ is used to denote the null eigenvector of the acoustic tensor $K_{ijkl} k_k^{(\alpha)} k_l^{(\alpha)}$, then the amplitude vectors must be of the form

$$A_j^{(\alpha)} = A^{(\alpha)} q_j^{(\alpha)} \tag{20}$$

for some scalar amplitudes $A^{(\alpha)}$. Finally, the traction-free boundary conditions (4), with $v_i = \delta_{1i}$, furnish the supplementary conditions

$$\sum_{\alpha=1}^{3} [K_{1jkl} k_k^{(\alpha)} q_l^{(\alpha)}] A^{(\alpha)} = 0. \tag{21}$$

This is a system of three equations with matrix of coefficients

$$M_{j\alpha} = K_{1jkl} k_k^{(\alpha)} q_l^{(\alpha)}. \tag{22}$$

For (21) to have non-trivial solutions, the condition

$$\det(\mathbf{M}) = 0 \tag{23}$$

must be satisfied. The localization orientations are specified by the unit vectors $\mathbf{n}^{(\alpha)}$ pointing in the direction of $\mathscr{R}e\,(\mathbf{k}^{(\alpha)})$.

*Stoneley waves*

Next we consider two dissimilar solids each occupying a half-space and bonded along the plane $x_1 = 0$. Consider Stoneley wave solutions of the type

$$v_j^+ = A_j^+ \exp\left[\mathrm{i}(k_k^+ x_k - \kappa^+ ct)\right], \quad v_j^- = A_j^- \exp\left[\mathrm{i}(k_k^- x_k - \kappa^- ct)\right] \tag{24}$$

where $(\,)^+$ and $(\,)^-$ denote the two sides of the interface. Here we write $(\kappa^\pm)^2 = (k_2^\pm)^2 + (k_3^\pm)^2$. For these solutions to decay exponentially into the body, the conditions

$$\mathscr{I}m\, k_1^- \leqslant 0, \quad \mathscr{I}m\, k_1^+ \geqslant 0 \tag{25}$$

need to be satisfied.

We now look for stationary wave solutions with $c = 0$. Substituting the stationary form of (24) into (3) results in

$$A_i^+ k_k^+ k_i^+ K_{ijkl}^+ = 0, \quad A_i^- k_k^- k_i^- K_{ijkl}^- = 0 \tag{26}$$

which admit non-trivial solutions provided that

$$\det\left[k_k^+ k_i^+ K_{ijkl}^+\right] = 0, \quad \det\left[k_k^- k_i^- K_{ijkl}^-\right] = 0. \tag{27}$$

As in the case of surface waves, $k_1^\pm$ may now be complex, due to the one-sided character of the solutions. Assume that for fixed $\kappa$ there are six complex solutions of (27), say $k_1^{(\alpha)\pm}$, $\alpha = 1, 2, 3$, compatible with (25). Let $A_j^{(\alpha)\pm}$, $\alpha = 1, 2, 3$, be the corresponding amplitudes. Then, the general form of the solution is

$$v_j^\pm = \sum_{\alpha=1}^{3} A_j^{(\alpha)\pm} \exp\left[\mathrm{i}(k_k^{(\alpha)\pm} x_k - \kappa^{(\alpha)\pm} ct)\right]. \tag{28}$$

Furthermore, the amplitudes $A_j^{(\alpha)}$ must be consistent with (26). Let $q_i^{(\alpha)\pm}$ be the null eigenvector of the acoustic tensors $K_{ijkl}^\pm k_k^{(\alpha)\pm} k_i^{(\alpha)\pm}$. Then, the amplitude vectors must be of the form

$$A_j^{(\alpha)\pm} = A^{(\alpha)\pm} q_j^{(\alpha)\pm}. \tag{29}$$

The relevant boundary conditions are continuity of velocity and traction rate at each point along the interface. Continuity requires

$$k_2^- = k_2^+, \quad k_3^- = k_3^+ \tag{30}$$

which in turn gives $\kappa^- = \kappa^+$. Using (29), the boundary conditions at the interface take the form

$$\begin{aligned} \sum_{\alpha=1}^{3} q_i^{(\alpha)-} A^{(\alpha)-} &= \sum_{\alpha=1}^{3} q_i^{(\alpha)+} A^{(\alpha)+} \\ \sum_{\alpha=1}^{3} \left[K_{1jkl}^- k_k^{(\alpha)-} q_l^{(\alpha)-}\right] A^{(\alpha)-} &= \sum_{\alpha=1}^{3} \left[K_{1jkl}^+ k_k^{(\alpha)+} q_l^{(\alpha)+}\right] A^{(\alpha)+}. \end{aligned} \tag{31}$$

This is a system of six equations for the six unknowns $A^{(\alpha)\pm}$. The matrix of coefficients of this system is given by

$$\begin{aligned} M_{i\alpha} &= q_i^{(\alpha)-}, \quad M_{(i+3)\alpha} = -q_i^{(\alpha)+} \\ M_{i(\alpha+3)} &= K_{1jkl}^- k_k^{(\alpha)-} q_l^{(\alpha)-}, \quad M_{(i+3)(\alpha+3)} = -K_{1jkl}^+ k_k^{(\alpha)+} q_l^{(\alpha)+}. \end{aligned} \tag{32}$$

For (31) to have non-trivial solutions, the matrix of coefficients must necessarily be singular, i.e.

$$\det(\mathbf{M}) = 0. \tag{33}$$

The localization orientations are specified by the unit vectors $\mathbf{n}^{(\alpha)\pm}$ pointing in the direction of $\mathscr{R}e\,(\mathbf{k}^{(\alpha)\pm})$.

## 4. STATIONARY WAVES IN PLANE STRAIN FOR INCOMPRESSIBLE SOLIDS OBEYING NORMALITY

We specialize the general approach in Section 3 to orthotropic solids deforming in plane strain, with in-plane loading coaxial to the $x_1$ and $x_2$ directions, so that $\sigma_{12} = 0$. The formulation takes a particularly simple form for the case of an incompressible solid, although incompressibility does necessitate a slight modification to the general framework. Furthermore, attention is restricted to solids having instantaneous moduli that possess the symmetries $K_{ijkl} = K_{klij}$. For elastic–plastic solids these symmetries are implied by plastic normality, i.e. coincidence of the loading and yield surfaces, in work conjugate variables. Defining $\sigma_{11} = \sigma_1$ and $\sigma_{22} = \sigma_2$, the tensor of in-plane instantaneous moduli can be written in the form given by Hill and Hutchinson (1975), where

$$K_{1111} = \mu_* - \sigma_1 \quad K_{1122} = \mu_* \quad K_{1112} = K_{1121} = 0 \tag{34}$$

$$K_{2211} = \mu_* \quad K_{2222} = \mu_* - \sigma_2 \quad K_{2212} = K_{2221} = 0 \tag{35}$$

$$K_{1212} = \mu + \frac{\sigma}{2} \quad K_{1221} = \mu - \sigma_m \quad K_{2121} = \mu - \frac{\sigma}{2} \tag{36}$$

with

$$\sigma_m = \tfrac{1}{2}(\sigma_1 + \sigma_2), \quad \sigma = (\sigma_1 - \sigma_2). \tag{37}$$

Shear-band, surface-wave and interface instabilities have been analyzed for this class of materials by Hill and Hutchinson (1975), Young (1976) and Steif (1986). The analyses here illustrate in an explicit fashion the identity of conditions for stationary waves and those governing the onset of shear banding.

*Stationary body waves*

The velocities and the hydrostatic stress rate are written in the form

$$v_j = A_j \exp[\mathrm{i}(k_k x_k - \kappa c t)] \quad \dot{p} = \mathrm{i} f \exp[\mathrm{i}(k_k x_k - \kappa c t)]. \tag{38}$$

Because of the incompressibility constraint, (9), the amplitudes, $A_j$, must satisfy

$$A_j k_j = 0. \tag{39}$$

The condition for stationary body waves is obtained by substituting (38) with $c = 0$ into (11). From (39)

$$A_2 = -A_1 \frac{k_1}{k_2} \tag{40}$$

and with $\mathbf{K}$ given by (34) to (36), the two in-plane equilibrium equations become

$$k_1 f + A_1 k_1^2 \left[2\mu_* - \mu - \frac{\sigma}{2}\right] + A_1 k_2^2 \left[\mu - \frac{\sigma}{2}\right] = 0$$

$$k_2^2 f + A_1 k_1 k_2^2 \left[\mu - 2\mu_* - \frac{\sigma}{2}\right] - A_1 k_1^3 \left[\mu + \frac{\sigma}{2}\right] = 0. \tag{41}$$

Eliminating $f$ gives

$$A_1 \left\{a^4 \left[\mu + \frac{\sigma}{2}\right] + 2a^2[2\mu_* - \mu] + \left[\mu - \frac{\sigma}{2}\right]\right\} = 0 \tag{42}$$

where $a = k_1/k_2$. For non-trivial solutions to exist, the term in brackets in (42) must vanish. Real values of $a$ that satisfy (42) give the orientation of stationary body waves. Three possibilities can be identified; (i) no real solutions exist; (ii) two real solutions exist; and (iii) four real solutions exist. These are termed by Hill and Hutchinson (1975) the elliptic, parabolic and hyperbolic regimes, respectively.

*Stationary Rayleigh waves*

Consider a solid extending over the half-space $x_1 \geqslant 0$, with zero prescribed tractions along $x_1 = 0$. Hence, $\sigma_1 = 0$ and $\sigma_2 = \pm|\sigma|$ in the current state. Analogous to (19), we consider wave solutions of the form:

$$v_j = \sum_{\alpha=1}^{2} A_j^{(\alpha)} \exp\left[\mathrm{i}(k_k^{(\alpha)} x_k - \kappa^{(\alpha)} c t)\right] \quad \dot{p} = \mathrm{i} \sum_{\alpha=1}^{2} f^{(\alpha)} \exp\left[\mathrm{i}(k_k^{(\alpha)} x_k - \kappa^{(\alpha)} c t)\right] \tag{43}$$

where $\alpha = 1, 2$. Solutions are sought that are periodic in $x_2$, with wavelength $\lambda = 2\pi/k_2$. Hence, $k_2$ is real and $k_2^{(1)} = k_2^{(2)} = k_2$. Furthermore, since there is nothing in the problem formulation to set the wavelength along the free surface, all units of length can be normalized with respect to the wavelength $\lambda$.

Define $a^{(\alpha)}$ as the ratio $k_1^{(\alpha)}/k_2$. Then, substituting (43) with $c = 0$ into the two momentum balance equations and eliminating the pressure term gives:

$$[a^{(\alpha)}]^4 \left[\mu + \frac{\sigma}{2}\right] + 2[a^{(\alpha)}]^2[2\mu_* - \mu] + \left[\mu - \frac{\sigma}{2}\right] = 0. \tag{44}$$

Equation (44) is simply the term in brackets in (42). When Rayleigh waves are possible in the elliptic regime, the four solutions to (44) are either a pair of complex conjugates or pure imaginary numbers. The only two roots that are relevant are those for which the real part of $\mathrm{i}k_1^{(\alpha)} = k_2 a^{(\alpha)}$ is negative so that the solution decays into the material. The orientation of the surface instability is given by $\mathscr{R}e\,(a^{(\alpha)})$. When $\mathscr{R}e\,(a^{(\alpha)}) = 0$ the localization is orthogonal to the free surface. Substituting (43) into the two boundary conditions along $x_1 = 0$,

$$[2\mu_* - \sigma_1] v_{1,1} + \dot{p} = 0 \tag{45}$$

and

$$[\mu - \sigma_m] v_{1,2} + \left[\mu + \frac{\sigma}{2}\right] v_{2,1} = 0 \tag{46}$$

gives

$$\begin{bmatrix} [\mu-\sigma_m]-[a^{(1)}]^2\left[\mu+\frac{\sigma}{2}\right] & [\mu-\sigma_m]-[a^{(2)}]^2\left[\mu+\frac{\sigma}{2}\right] \\ a^{(1)}[4\mu_*-\mu-\sigma_m]+[a^{(1)}]^3\left[\mu+\frac{\sigma}{2}\right] & a^{(2)}[4\mu_*-\mu-\sigma_m]+[a^{(2)}]^3\left[\mu+\frac{\sigma}{2}\right] \end{bmatrix} \begin{pmatrix} A_1^{(1)} \\ A_1^{(2)} \end{pmatrix} = 0. \tag{47}$$

A non-trivial solution requires the determinant of coefficients in (47) to vanish. In the elliptic regime, this requires

$$4\mu_*-2\sigma_m = \frac{\sigma_m^2-2\mu\sigma_m+\frac{1}{4}\sigma^2}{\mu-\sigma/2}\sqrt{\frac{\mu-\sigma/2}{\mu+\sigma/2}}. \tag{48}$$

Setting $\sigma_m/\sigma = -1/2$ and $\sigma_m/\sigma = 1/2$ in (48) gives the surface wave bifurcation conditions of Hill and Hutchinson (1975) for tension, and Young (1976) for compression, respectively. The values of stress and moduli determined from (48) are substituted into (44) to determine the $a^{(\alpha)}$ which give the orientation and decay length relative to the free-surface wavelength $\lambda$.

*Stationary Stoneley waves*

We consider two materials characterized by a constitutive relation of the form (13)–(15) bonded along $x_1 = 0$. Quantities associated with the material occupying the region $x_1 > 0$ are denoted by + and those associated with the material occupying the region $x_1 < 0$ are denoted by −. In each half-space, the current state is presumed to be one of homogeneous tension or compression. For $x_1 > 0$, $\sigma_{11} = \sigma_1^+$, $\sigma_{22} = \sigma_2^+$ and $\sigma_{12} = 0$. Correspondingly, for $x_1 < 0$, $\sigma_{11} = \sigma_1^-$, $\sigma_{22} = \sigma_2^-$ and $\sigma_{12} = 0$. Equilibrium in the current state requires $\sigma_1^+ = \sigma_1^- = \sigma_1$.

Now solutions are sought of the form

$$v_1^\pm = \sum_{\alpha=1}^{2} A^{(\alpha)\pm} \exp\left[\mathrm{i}(k_1^{(\alpha)\pm}x_1 + k_2x_2)\right] \tag{49}$$

$$v_2^\pm = \sum_{\alpha=1}^{2} -A^{(\alpha)\pm}k_1^{(\alpha)\pm} \exp\left[\mathrm{i}(k_1^{(\alpha)\pm}x_1 + k_2x_2)\right] \tag{50}$$

$$\dot{p}^\pm = \mathrm{i}\sum_{\alpha=1}^{2} f^{(\alpha)\pm} \exp\left[\mathrm{i}(k_1^{(\alpha)\pm}x_1 + k_2x_2)\right] \tag{51}$$

where $\mathscr{R}e\,(\mathrm{i}k_1^{(\alpha)+}) < 0$ and $\mathscr{R}e\,(\mathrm{i}k_1^{(\alpha)-}) > 0$.

The four coefficients $A^{(\alpha)\pm}$ are obtained from the boundary conditions along the interface which are

$$v_1^+(0,x_2) = v_1^-(0,x_2) \quad v_2^+(0,x_2) = v_2^-(0,x_2) \tag{52}$$

$$\dot{t}_{11}^+ = \dot{t}_{11}^- \quad \dot{t}_{12}^+ = \dot{t}_{12}^-. \tag{53}$$

Substituting (49) through (51) into (52) and (53), using the momentum balance equations for $x_1 > 0$ and $x_1 < 0$ to eliminate $f^{(\alpha)\pm}$, and introducing $a^{(\alpha)\pm} = k_1^{(\alpha)\pm}/k_2$, gives four equations for the four unknowns $A^{(\alpha)\pm}$, $\alpha = 1, 2$. These equations can be written in the form

$$\begin{bmatrix} 1 & 1 & -1 & -1 \\ a^{(1)+} & a^{(2)+} & -a^{(1)-} & -a^{(2)-} \\ M_{31} & M_{32} & M_{33} & M_{34} \\ M_{41} & M_{42} & M_{43} & M_{44} \end{bmatrix} \begin{bmatrix} A^{(1)+} \\ A^{(2)+} \\ A^{(1)-} \\ A^{(2)-} \end{bmatrix} = 0 \tag{54}$$

where

$$M_{31} = [\mu^+ - \sigma_m^+] - [\mu^+ + \sigma^+/2][a^{(1)+}]^2 \tag{55}$$

$$M_{32} = [\mu^+ - \sigma_m^+] - [\mu^+ + \sigma^+/2][a^{(2)+}]^2 \tag{56}$$

$$M_{33} = -[\mu^- - \sigma_m^-] + [\mu^- + \sigma^-/2][a^{(1)-}]^2 \tag{57}$$

$$M_{34} = -[\mu^- - \sigma_m^-] + [\mu^- + \sigma^-/2][a^{(2)-}]^2 \tag{58}$$

$$M_{41} = [4\mu_*^+ - \mu^+ - \sigma_m^+][a^{(1)+}] + [\mu^+ + \sigma^+/2][a^{(1)+}]^3 \tag{59}$$

$$M_{42} = [4\mu_*^+ - \mu^+ - \sigma_m^+][a^{(2)+}] + [\mu^+ + \sigma^+/2][a^{(2)+}]^3 \tag{60}$$

$$M_{43} = -[4\mu_*^- - \mu^- - \sigma_m^-][a^{(1)-}] - [\mu^- + \sigma^-/2][a^{(1)-}]^3 \tag{61}$$

$$M_{44} = -[4\mu_*^- - \mu^- - \sigma_m^-][a^{(2)-}] - [\mu^- + \sigma^-/2][a^{(2)-}]^3. \tag{62}$$

Setting the determinant of the matrix of coefficients in (54) equal to zero in the elliptic regime implies

$$\begin{aligned} &(a^{(1)+} - a^{(2)+})(a^{(1)-} - a^{(2)-})\{[(\mu^+ - \mu^-) - (\sigma_m^+ - \sigma_m^-)]^2 \\ &- [\sqrt{(\mu^+)^2 - (\sigma^+)^2/4} - \sqrt{(\mu^-)^2 - (\sigma^-)^2/4}]^2 \\ &- [\sqrt{(\mu^+)^2 - (\sigma^+)^2/4} - \sqrt{(\mu^-)^2 - (\sigma^-)^2/4}][4(\mu_*^+ - \mu_*^-) - 2(\sigma_m^+ - \sigma_m^-)] \\ &- [(4\mu_* - 2\mu^-)\sqrt{(\mu^+)^2 - (\sigma^+)^2/4} + (4\mu_*^+ - 2\mu^+)\sqrt{(\mu^-)^2 - (\sigma^-)^2/4}] \\ &+ [(\mu^+ + \sigma^+/2)\sqrt{(\mu^-)^2 - (\sigma^-)^2/4} + (\mu^- + \sigma^-/2)\sqrt{(\mu^+)^2 - (\sigma^+)^2/4}]K\} = 0 \end{aligned} \tag{63}$$

where

$$K = -\left[\frac{(4\mu_*^+ - 2\mu^+)}{(\mu^+ + \sigma^+/2)} + 2\sqrt{\frac{\mu^+ - \sigma^+/2}{\mu^+ + \sigma^+/2}}\right]^{1/2}\left[\frac{(4\mu_*^- - 2\mu^-)}{(\mu^- + \sigma^-/2)} + 2\sqrt{\frac{\mu^- - \sigma^-/2}{\mu^- + \sigma^-/2}}\right]^{1/2}. \tag{64}$$

Equilibrium requires $\sigma_1^+ = \sigma_1^-$ so that both $(\sigma^+ - \sigma^-)$ and $(\sigma_m^+ - \sigma_m^-)$ only involve the jump in $\sigma_2$. Clearly, since the material on both sides of the interface is incompressible, the critical condition for bifurcation is independent of a superposed hydrostatic stress.

When a solution satisfying (63) is found, the band orientation and decay length are given by the real and imaginary parts of $k_1^{(\alpha)+}$ and $k_1^{(\alpha)-}$ for $x_1 > 0$ and $x_1 < 0$, respectively, from equations of the form (44), with coefficients given by moduli and stress values for the appropriate region. In general both the band orientation and decay length differ on each side of the interface.

## 5. PLANAR CRYSTALLINE SOLIDS

A specific constitutive relation that gives rise to moduli of the type (34)–(36) is the planar double-slipping model of Asaro (1979), when oriented for symmetric double slip.

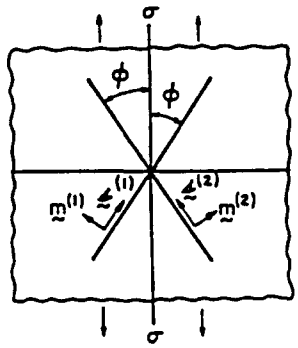


Fig. 1. Schematic of the plane strain model for a single crystal undergoing double slip.

The geometry of this model crystal is shown in Fig. 1. For slip on a single system, the slip rate, $\dot{\gamma}$, is given by $\dot{\gamma} = \dot{\tau}/h$, where $\tau$ is the Schmid resolves shear stress and $h$ is the self-hardening. For a deformation history of continued symmetric double slip, $\tau$ and $\gamma$ are related to the principal stresses and strains by

$$\tau = \frac{(\sigma_1 - \sigma_2)}{2} \sin(2\phi) \quad \gamma = \frac{(\varepsilon_1 - \varepsilon_2)}{\sin(2\phi)}. \tag{65}$$

In the second of (65), elastic straining has been neglected and the total strains have been identified with the plastic strains.

When the elasticity is taken to be volume preserving and when stress magnitude is small compared to the crystal's elastic shear modulus, the incremental moduli have the form (34)-(36) with (Asaro, 1979; Peirce *et al.*, 1982):

$$\mu_* = \frac{h(1+q)}{2\sin^2(2\phi)} \tag{66}$$

$$\mu = \frac{h(1-q) + (\sigma_1 - \sigma_2)\cos(2\phi)}{2\cos^2(2\phi)}. \tag{67}$$

The parameter $q$ describes the latent hardening, i.e. the increase in strength on one system due to slip on another. Here, the self-hardening $h$ is described by a power law function of the accumulated slip $\gamma$,

$$h(\gamma) = h_0 \left[\frac{h_0 \gamma}{n\tau_0} + 1\right]^{n-1} \tag{68}$$

where $\tau_0$ is the initial flow strength, $h_0$ is the initial hardening and $n$ is the strain hardening exponent. The latent hardening parameter $q$ is taken to be a specified constant. The material response depends sensitively on the angle $\phi$. We confine attention to the range $0 < \phi < \pi/4$, where both $\mu_*$ and $\mu$ are positive, and where there is a yield surface vertex at the current loading point, with the vertex angle $4\phi$. At $\phi = \pi/4$, the yield surface is smooth and at $\phi = 0$, the yield cone collapses to a line. Hence, increasing $\phi$ gives an increasing stiffness of the response.

This constitutive model has been used in Asaro (1979) and Peirce *et al.* (1982) to analyze shear band localizations in ductile single crystals. Peirce *et al.* (1982) also present some results on surface instabilities. Here, this constitutive relation is used to investigate yield surface vertex effects on interface instabilities. The aim is to illustrate the full range

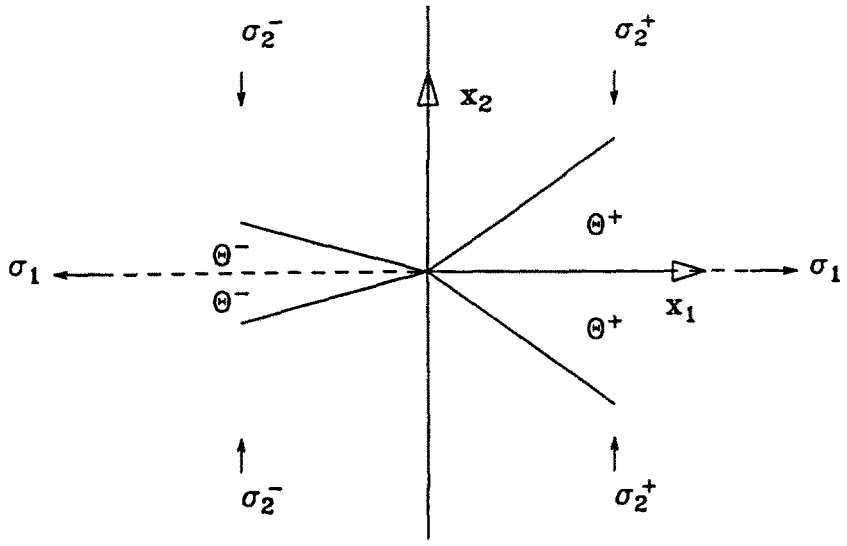


Fig. 2. Geometry of shear bands at a bicrystal interface.

of possible behaviors rather than to study actual crystal geometries. As sketched in Fig. 2 a model bicrystal interface is considered, where each "crystal" is taken to be oriented for symmetric double slip. For purposes of illustration, all the material properties in each half-space are taken to be identical except for the angle between slip systems $\phi$.

Since the current state is one of homogeneous deformation in each crystal and each crystal is incompressible, $\varepsilon_1 = -\varepsilon_2$ everywhere. Hence, continuity of displacement components across the interface together with homogeneity requires both $\varepsilon_1$ and $\varepsilon_2$ to have the same value in each crystal. However, the stress states in the two half-spaces differ because in general $\sigma_2^+ \neq \sigma_2^-$. We focus on circumstances where the loading normal to the interface is tensile $(\sigma_1 - \sigma_2) > 0$ and $\phi \leqslant 45^\circ$.

There are three possibilities: (i) a shear band localization occurs first in $x_1 > 0$; (ii) a shear band localization occurs first in $x_1 < 0$; and (iii) a localized interface instability occurs first. In the first two circumstances, because of the inhomogeneity in properties, the localization is at least initially confined to one half-space. Hence, the interface acts as a barrier to a localization that initiates in the bulk. In the third case, the interface acts as the initiation site for the instability.

Regimes illustrating these three possibilities can be distinguished in Fig. 3 where $h_0/\tau_0 = 10$, $n = 0.3$ and $q = 1$. The slip system angle $\phi$ is fixed at 15° in $x_1 > 0$ and variable in $x_1 < 0$. The critical value of $\varepsilon = \varepsilon_1 - \varepsilon_2$ at which various stationary waves are possible is plotted against $\Delta\phi = \phi(x_1 > 0) - \phi(x_1 < 0)$. When the material is nearly uniform, i.e.

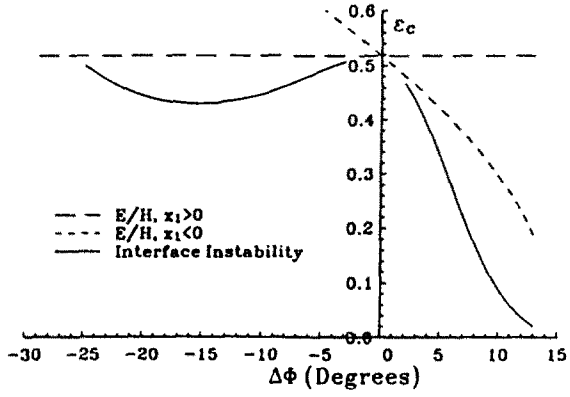


Fig. 3. The critical strain for bulk and interfacial localization as a function of the misorientation across the bicrystal interface. $\phi$ is fixed at 15° for $x_1 > 0$. $h_0/\tau_0 = 10$, $n = 0.3$ and $q = 1$.

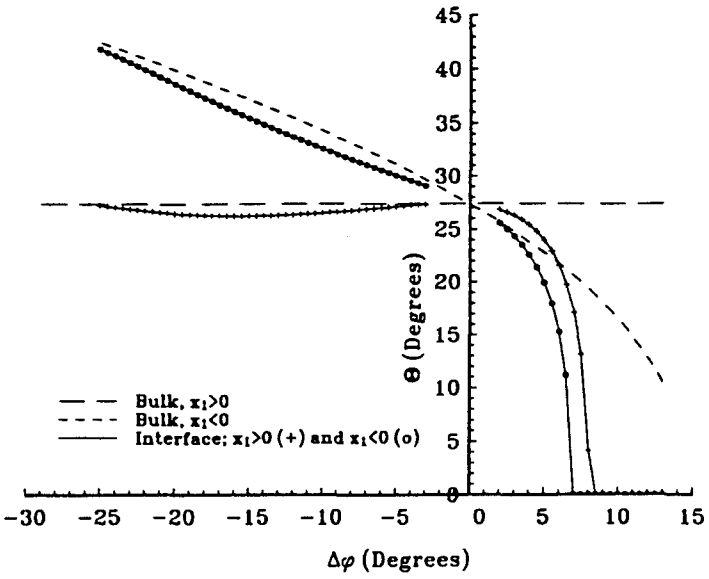


Fig. 4. The band orientation for bulk and interfacial localization as a function of the misorientation across the bicrystal interface. $\phi$ is fixed at 15° for $x_1 > 0$. $h_0/\tau_0 = 10$, $n = 0.3$ and $q = 1$. When the interface instability is critical the different band orientations on the two sides of the interface are shown.

$\Delta\phi \approx 0$, the behavior is like that for a homogeneous solid. Bulk localization occurs at nearly the same critical strain in both half-spaces and the interface plays a negligible role. For $\Delta\phi$ near $-30°$, $\phi^-$ is near 45°, which gives a very stiff response in $x_1 < 0$. In this regime, bulk localization occurs in the half-space $x_1 > 0$ and the interface acts as a barrier to localization. In the remaining range of $\Delta\phi$ an interface instability precedes bulk localization in either half-space. In the limit as $\Delta\phi \to 15°$, $\phi^- \to 0$, and from (66) and (67), $\mu_*/\mu \to \infty$. Here, an interface instability can occur at a much smaller strain than does bulk localization.

The localization orientation is shown as a function of $\Delta\phi$ in Fig. 4. Here, $\Theta$ measures the rotation of the band normal from the $x_2$ axis, as shown in Fig. 2. For any given critical strain, band orientations of both $+\Theta$ and $-\Theta$ occur. The dashed lines in Fig. 4 show the orientation of bulk shear bands in each of the two half-spaces. The solid lines show the orientations associated with the interface instability. For $\Delta\phi < 0$, the orientation of the interface localization in each half-space differs little from that of the corresponding bulk localization. However, note that in this regime the interface instability can still give rise to significantly different band orientations in $x_1 > 0$ and $x_1 < 0$. When $\Delta\phi = -3°$, the difference between the localization orientation in $x_1 > 0$ and $x_1 < 0$ is about 3°. This misorientation increases with increasing $|\Delta\phi|$ and reaches 12° at $\Delta\phi = -25°$. For smaller values of $\Delta\phi$ (larger absolute values), the interface instability is no longer critical. In the regime where $\Delta\phi > 0$ and the interface instability is critical, the localization orientation angles $\Theta^{\pm}$ decrease as $\Delta\phi$ is increased. First for $x_1 < 0$ and then on both sides of the interface, $\Theta = 0$. Vanishing $\Theta$ corresponds to pure imaginary $k_1^{(2)}$ in (49)-(51), which means that the fields simply decay exponentially away from the interface, without any oscillating part.

The (signed) decay length associated with the interface instability, normalized by the surface wavelength, is plotted against $\Delta\phi$ in Fig. 5. The decay length is given by $s^{(2)+} = 1/\mathcal{I}m(k_1^{(2)+})$ in $x_1 > 0$ and $s^{(2)-} = 1/\mathcal{I}m(k_1^{(2)-})$ in $x_1 < 0$, while the surface wavelength is $\lambda = 2\pi/k_2$. The longer the decay length the greater the distance the non-uniformity of deformation associated with the interface instability penetrates into the material. When the critical strain for the interface instability approaches the critical strain for bulk shear bands on one side of the interface, the decay length on that side becomes unbounded. For $\Delta\phi < 0$, in $x_1 > 0$, there is a broad range over which $s^{(2)+}/\lambda \approx 1$, the critical strain for the interface localization, is close to that for bulk shear bands. When $\Theta = 0$, i.e. when the roots

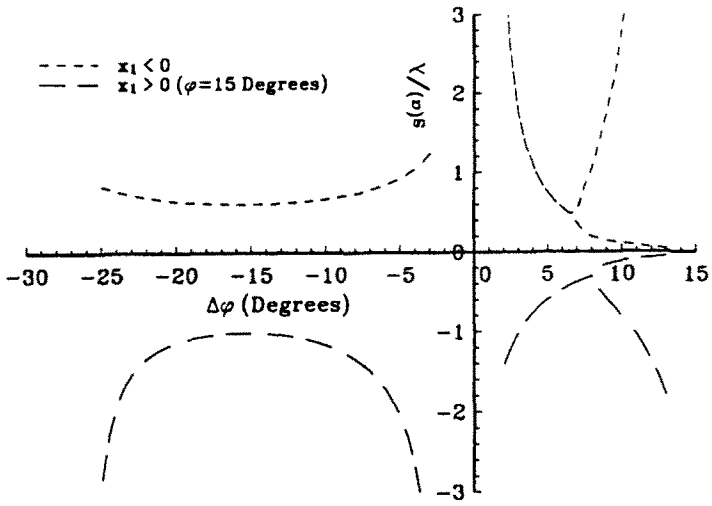


Fig. 5. The normalized decay length associated with the interface instability as a function of the misorientation across the bicrystal interface. $\phi$ is fixed at 15° for $x_1 > 0$. $h_0/\tau_0 = 10$, $n = 0.3$ and $q = 1$. $\lambda$ is the wavelength along the interface. The different band decay lengths on the two sides of the interface are shown.

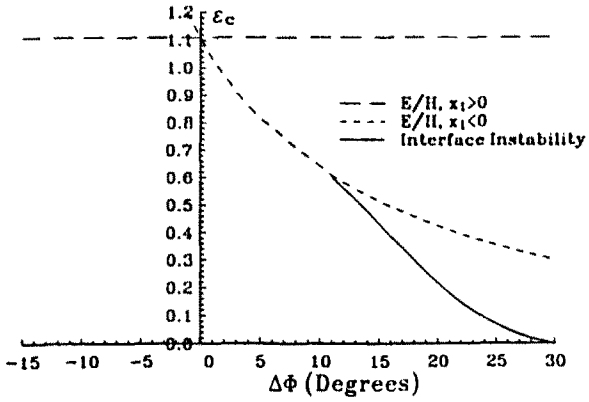


Fig. 6. The critical strain for bulk and interfacial localization as a function of the misorientation across the bicrystal interface. $\phi$ is fixed at 30° for $x_1 > 0$. $h_0/\tau_0 = 10$, $n = 0.3$ and $q = 1$.

to (44) become pure imaginary, there are two distinct decay lengths for a given value of $\Delta\phi$; one relatively short and one relatively long.

The value $\phi = 15°$ was chosen to illustrate a broad range of behavior and not to model any crystal geometry. The value $\phi = 30°$ is representative of a certain crystal geometry (Asaro, 1979; Peirce *et al.*, 1982), and Fig. 6 shows the critical strain for stationary Stoneley waves versus $\Delta\phi$ when $\phi$ is fixed at 30° for $x_1 > 0$. In this case, there is only a range of positive $\Delta\phi$ where an interface localization precedes bulk localization. The qualitative features of the solution in this range are as shown in Figs 4 and 5.

## 6. FRICTIONAL PRESSURE-SENSITIVE SOLIDS

For a broad class of elastic–plastic solids with smooth yield surfaces, the incremental moduli $L_{ijkl}$ in (12) are of the form

$$L_{ijkl} = L^e_{ijkl} - \frac{(L^e_{ijmn}P_{mn})(Q_{pq}L^e_{pqkl})}{h + L^e_{mnpq}P_{mn}Q_{pq}} \tag{69}$$

during plastic loading, where $L^e_{ijkl}$ are the incremental elastic moduli, $h$ is a plastic modulus and **P** and **Q** are unit tensors. Restricting attention to plane-strain deformations in the

plane $x_1-x_2$, and assuming the material to be incrementally orthotropic with principal directions of orthotropy and stress aligned with the coordinate axes, (12) reduces to

$$\begin{aligned} K_{1111} &= L_{1111}+\sigma_1, \quad K_{1122} = L_{1122} \\ K_{2222} &= L_{2222}+\sigma_2, \quad K_{2211} = L_{2211} \\ K_{1212} &= L_{1212}+\sigma_1, \quad K_{1221} = L_{1212} \\ K_{2121} &= L_{1212}+\sigma_2, \quad K_{2112} = L_{1212}. \end{aligned} \tag{70}$$

We shall further assume that the incremental elastic response is isotropic, so that $L^e_{ijkl}$ can be expressed in terms of two instantaneous Lamé constants $\lambda$ and $\mu$. In these circumstances, $L^e_{ijmn}P_{mn}$ and $Q_{pq}L^e_{pqkl}$ are diagonal in the adopted reference frame. Then, it follows that the in-plane components of $L^e_{ijmn}P_{mn}$ and $Q_{pq}L^e_{pqkl}$ can be represented in terms of a single parameter for each tensor. Here, we adopt a parameterization based on the Mohr–Coulomb model and write the moduli as

$$\begin{aligned} L_{1111} &= \lambda+2\mu-\frac{1}{D}[\mu+(\lambda+\mu)\tan\psi][\mu+(\lambda+\mu)\tan\phi] \\ L_{1122} &= \lambda-\frac{1}{D}[\mu+(\lambda+\mu)\tan\psi][-\mu+(\lambda+\mu)\tan\phi] \\ L_{2211} &= \lambda-\frac{1}{D}[-\mu+(\lambda+\mu)\tan\psi][\mu+(\lambda+\mu)\tan\phi] \\ L_{2222} &= \lambda+2\mu-\frac{1}{D}[-\mu+(\lambda+\mu)\tan\psi][-\mu+(\lambda+\mu)\tan\phi] \\ L_{1212} &= \mu \end{aligned} \tag{71}$$

where $\phi$ is the instantaneous angle of friction, $\psi$ the instantaneous dilatancy angle, and

$$D = h+\mu+(\lambda+\mu)\tan\phi\tan\psi. \tag{72}$$

We note that $L_{ijkl} \neq L_{klij}$ for solids lacking normality, i.e. when $\psi \neq \phi$. Tacit in (71) is the assumption that the smallest (most negative) principal stress corresponds to the $x_2$ axis. It bears emphasis that (71) furnishes a general parameterization of incremental moduli under the assumptions stated, namely overall orthotropy of the solid, isotropy of the incremental elastic moduli and smooth yield surface. Corner effects can be accounted for by replacing the elastic value of $\mu$ given to $L_{1212}$ in (71) by an independent modulus $\mu' \leqslant \mu$, but this possibility is not pursued here. An example of a solid whose constitutive behavior exhibits corner effects is developed in Section 5.

*Stationary body waves*

Inserting (71) into the localization condition (16) gives

$$Aa^4+Ba^2+C=0 \tag{73}$$

where

$$\begin{aligned} A &= -(\mu+\sigma_2)\{(\lambda+\mu)\mu(1+\tan\phi)(1+\tan\psi)+(\lambda+2\mu)h+D\sigma_2\} \\ C &= -(\mu+\sigma_1)\{(\lambda+\mu)\mu(1-\tan\phi)(1-\tan\psi)+(\lambda+2\mu)h+D\sigma_1\} \\ B &= \frac{A+C}{2}+2(\lambda+\mu)\mu^2-\frac{\sigma_1-\sigma_2}{2}\{2(\lambda+\mu)\mu(\tan\phi+\tan\psi)-D(\sigma_1-\sigma_2)\}. \end{aligned} \tag{74}$$

The elliptic–hyperbolic boundary is defined by the condition $B^2-4AC=0$, which can be used to determine the critical value $h_c$ of the plastic modulus. If $\sigma_1$ and $\sigma_2$ are neglected in (74), it is possible to solve (73) for $h_c$ explicitly, with the result

$$\frac{h_c}{\mu}=\frac{\lambda+\mu}{4(\lambda+2\mu)}(\tan\phi-\tan\psi)^2. \tag{75}$$

The corresponding band orientations are

$$a^{(1,2)}=\pm\left[\frac{1+(\tan\phi+\tan\psi)/2}{1-(\tan\phi+\tan\psi)/2}\right]^{1/2}. \tag{76}$$

These values are double roots of (73) and define two band orientations symmetrically disposed relative to the stress axis.

With the interpretation given above to $\phi$ and $\psi$, as the instantaneous friction and dilatancy angles at the current state, (75) generalizes the results of Rudnicki and Rice (1975) derived for a specific Drucker–Prager-like model. In particular, we note that, under conditions of lack of normality, $\psi\neq\phi$, localization can occur with positive hardening. As noted by Rudnicki and Rice (1975), neglecting the geometric stress terms in (70) gives results which are correct to first order in the ratio between the stress components and the elastic moduli.

*Stationary Rayleigh waves*

With $\sigma_1$ and $\sigma_2$ neglected in (70), the critical value of $h$ for the emergence of stationary Rayleigh waves is $h_c=0$. Thus, boundary shear bands necessarily occur at the peak stress, to within first-order terms in the ratio of stress to elastic moduli. In particular, when $\phi\neq\psi$ and the stress–strain curve is concave-up, so as to give a monotonically decreasing $h$, localization in the bulk of the solid always precedes localization at the boundary. To the same order of approximation, the orientation $a=k_1/k_2$ of the surface bands may take the following values

$$a^{(1,2)}=\pm\left(\frac{1+\tan\psi}{1-\tan\psi}\right)^{1/2},\quad a^{(3,4)}=\pm\left(\frac{1+\tan\phi}{1-\tan\phi}\right)^{1/2} \tag{77}$$

at $h_c$. These correspond to four distinct roots of (73).

Because the stationary Rayleigh waves became available in the hyperbolic regime, the four roots of (73) are real at $h_c$ and, hence, trivially satisfy the decay condition (18). Solutions can be sought in the form of combinations of two or more of the four admissible waves as in (19). Here we have confined attention to pairwise combinations of waves. Three such combinations are found to satisfy (23): (a) $a^{(1)}$ and $a^{(2)}$; (b) $a^{(1)}$ and $a^{(3)}$; and (c) $a^{(1)}$ and $a^{(4)}$. Solution (a) is symmetric about the $x_1$ axis, whereas solutions (b) and (c) are unsymmetric, Fig. 7. For a plastically incompressible material, $\psi=0$, solution (a) corresponds to two bands intersecting the boundary at 45°. In addition, solutions (a) and (c) exhibit one band on each side of the $x_1$ axis, whereas solution (b) corresponds to two bands lying on the same side of the $x_1$ axis, Fig. 7.

Comparison of (76) and (77) reveals that bands in the bulk and at the surface of the solid are generally misaligned. For pressure-sensitive frictional materials, this misalignment can have a marked effect on the global response of a solid. Consider, for example, the case of a rectangular soil sample tested in plane strain compression, as sketched in Fig. 8a. With $\psi\neq\phi$, shear banding will tend to initiate in the interior of the solid during the ascending portion of the force–elongation curve, and, at the peak load, will connect to the free boundary. However, the orientation of the interior and surface shear bands can differ substantially. For instance, for the plastically-incompressible solid, the symmetric surface shear bands are at 45° to the axis of loading, whereas the interior shear band can be

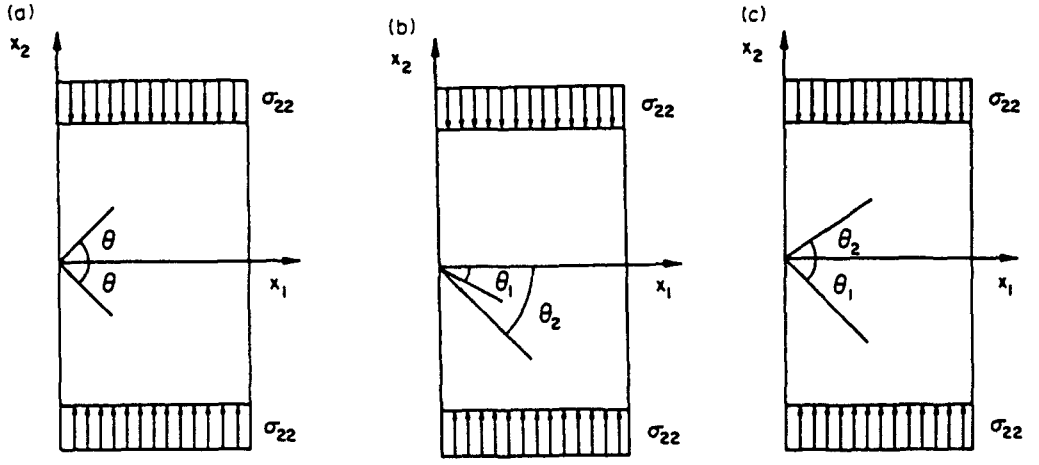


Fig. 7. Geometry of shear bands intersecting a free surface.

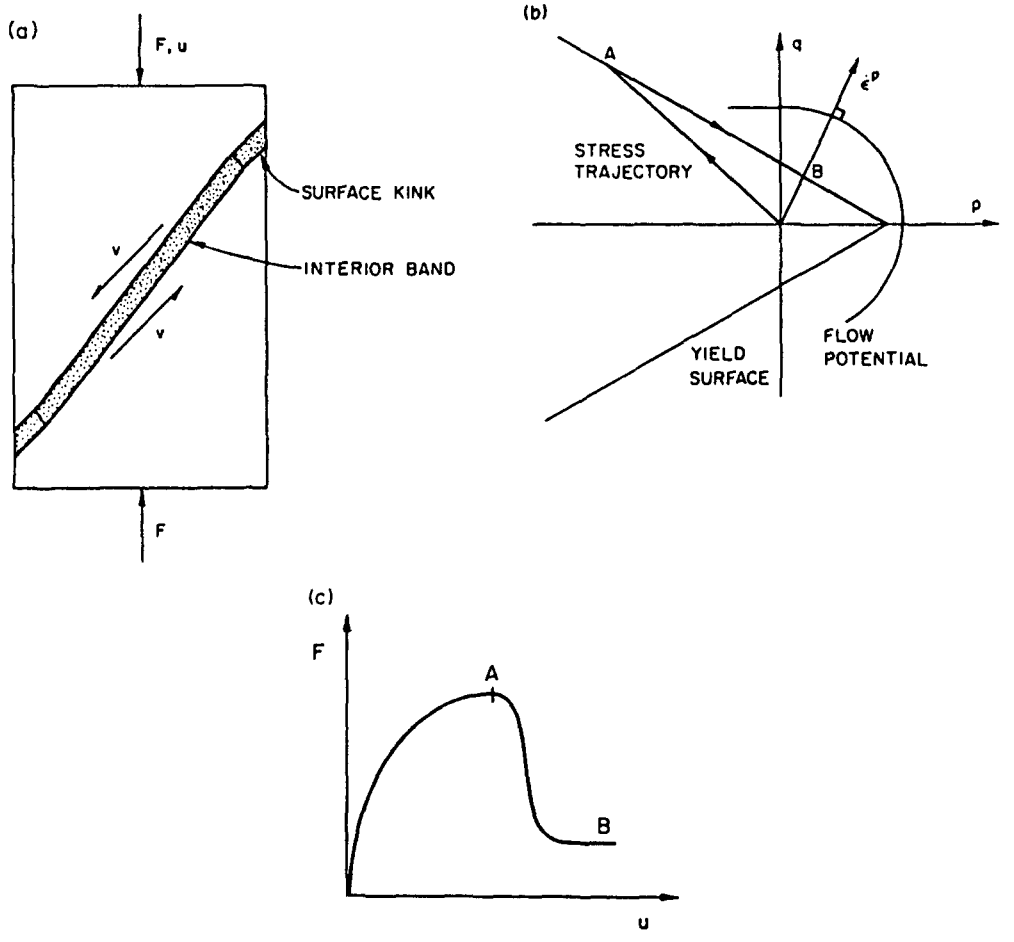


Fig. 8. The role of orientation mismatch between interior and surface shear bands in pressure-sensitive dilatant materials. (a) Shear band geometry exhibiting surface kinks. (b) Stress trajectories in the plane strain compression test. (c) Resulting force versus elongation curve.

significantly steeper. Indeed, finite element simulations of the plane strain compression test in soils invariably exhibit "kinks" in the shear bands as they connect to the boundary (Leroy and Ortiz, 1989, 1990).

As is evident from Fig. 8a, the relative motion of the unloaded blocks is determined

by the orientation of the surface bands. Because of the orientation mismatch, the bulk band must necessarily dilate as it shears. In frictional pressure-sensitive materials, for any substantial dilation to be possible the state of stress must necessarily be on the hydrostatic tension cap of the flow potential, Fig. 8b. But, because of the pressure-sensitive nature of yield, the tension cap can only be reached at the expense of a sharp drop in the level of stress, which is reduced to values of the order of the cohesion of the solid, Fig. 8b. Consequently, a typical force–elongation diagram has the general form shown in Fig. 8c. Following an initial hardening stage, a sharp drop in the bearing capacity of the specimen ensues as the shear band reaches the free surface, thereafter stabilizing at a lower plateau. This type of behavior has been experimentally observed in soils by Vardoulakis and Graf (1985), and is also a common occurrence in rocks (Waversik and Brace, 1971) and concrete (van Mier, 1984).

## 7. SUMMARY AND DISCUSSION

Here we have argued that the emergence of general stationary wave solutions, exemplified by Rayleigh surface waves and Stoneley interface waves, signals the onset of localization, in much the same manner as the existence of stationary body waves is a necessary condition for localization in the interior of a rate-independent solid. Furthermore, the stationary-wave solutions yield the possible orientations of the emerging shear bands. For instance, an investigation of stationary Rayleigh and Stoneley waves has enabled us to determine critical conditions for the inception of localization at a free boundary and at a material interface, respectively, and to compute the orientations of the corresponding shear bands. While these stationary-wave solutions generally correspond to the onset of an instability, their shear-band interpretation is restricted to the immediate vicinity of the surface or interface when they precede bulk localization.

It should be noted that since there is nothing in the present formulation that defines a length scale, the wavelength of the stationary Rayleigh and Stoneley waves is arbitrary. Other lengths, i.e. decay lengths into the bulk material, are determined relative to this wavelength. However, the general framework does carry over to circumstances where there is a material characteristic length (Zbib and Aifantis, 1988), or an interface characteristic length (Suo *et al.*, 1991).

We have found that grain boundaries in polycrystals can act as both barriers to, and sources of, shear bands. This is because, depending on the prevailing conditions, localization may occur in the interior first, followed by localization at the interface, or, conversely, localization may start at the interface followed by localization in the interior. A key constitutive feature which makes this dual role of interfaces possible is the corner-like behavior of plastic flow in crystals. In some metals, shear bands which arrest at grain boundaries may nucleate interfacial microcracks which contribute to a brittle mode of failure. More generally, the ability of shear bands to cross grain boundaries may markedly influence the overall ductility of the solid.

A similar analysis of pressure-sensitive frictional materials reveals a mismatch in orientation between the shear bands in the interior and on the boundary of the solid. In rectangular samples tested in plane strain compression, this mismatch results in dilation in the interior band, which in turn causes a precipitous loss of bearing capacity of the specimen. Whereas this phenomenon had been extensively documented in the experimental and computational literature on granular media, a complete mechanistic explanation was lacking. Drescher and Vardoulakis (1982) had surmised that the apparent softening of sand samples in plane strain compression is related to shear banding, but the role of surface "kink bands" as the sources of dilatation in the interior band was not identified. In fact, an infinite-band analysis carried out by Leroy and Ortiz (1989) shows that the failure to consider the surface kink results in a severe underestimation of the load drop which follows localization. The implication of these observations as regards constitutive modelling is that the apparent softening which is observed experimentally cannot be construed as a constitutive feature but, instead, is the result of the complex structural response of the sample.

It would appear that the usefulness of the stationary-wave analysis extends beyond the

specific examples treated in this paper. The particular case of stationary body waves, the study of which was pioneered by Hadamard (1903), Hill (1962), Mandel (1966) and Rice (1977), has proven of great value in elucidating how various constitutive features influence localization in the interior of solids. Much in the same spirit, the analysis of general stationary waves provides an equally-useful tool for undertaking a systematic study of localization instabilities under more general conditions.

*Acknowledgements*—We are grateful for the support provided by the Brown University Materials Research Group on Plasticity and Fracture, funded by the National Science Foundation. Algebraic manipulations in Section 4 were facilitated through use of *Mathematica* from Wolfram Research Inc.

## REFERENCES

Asaro, R. J. (1979). Geometrical effects in the inhomogeneous deformation of ductile single crystals. *Acta Metall.* **27**, 445–453.

Benallal, A., Billardon, R. and Geymonat, G. (1989). Some mathematical aspects of the damage-softening rate problem. In *Cracking and Damage—Strain Localization and Size Effect* (Edited by J. Mazars and Z. P. Bazant), pp. 247–258. Elsevier, Amsterdam.

Biot, M. A. (1963a). Internal buckling under initial stress in finite elasticity. *Proc. R. Soc. London* **A273**, 306–328.

Biot, M. A. (1963b). Surface instability in finite anisotropic elasticity under initial stress. *Proc. R. Soc. London* **A273**, 329–339.

Biot, M. A. (1963c). Interfacial instability in finite elasticity under initial stress. *Proc. R. Soc. London* **A273**, 340–344.

Dowaikh, M. A. and Ogden, R. W. (1990). On surface waves and deformations in a pre-stressed incompressible elastic solid. *IMA J. Appl. Math.* **44**, 261–284.

Drescher, A. and Vardoulakis, I. (1982). Geometric softening in triaxial tests on granular material. *Géotechnique* **32**, 291–303.

Hadamard, J. (1903). *Leçons sur la Propagation des Ondes et les Équations de L'Hydrodynamique*, Chap. 6. Hermann, Paris.

Hill, R. (1958). A general theory of uniqueness and stability in elastic–plastic solids. *J. Mech. Phys. Solids* **6**, 236–249.

Hill, R. (1962). Acceleration waves in solids. *J. Mech. Phys. Solids* **10**, 1–16.

Hill, R. and Hutchinson, J. W. (1975). Bifurcation phenomena in the plane tensile test. *J. Mech. Phys. Solids* **23**, 239–264.

Hutchinson, J. W. and Tvergaard, V. (1980). Surface instabilities on statically strained plastic solids. *Int. J. Mech. Sci.* **22**, 339–354.

Leroy, Y. and Ortiz, M. (1989). Finite element analysis of transient strain localization phenomena in frictional solids. *Int. J. Num. Anal. Meth. Geomech.* **14**, 53–74.

Leroy, Y. and Ortiz, M. (1990). Finite element analysis of strain localization in frictional solids. *Int. J. Num. Anal. Meth. Geomech.* **14**, 93–124.

Mandel, J. (1966). Conditions de stabilité et postulat de Drucker. In *Rheology and Soil Mechanics* (Edited by J.Kravtchenko and P. M. Sirieys), pp. 58–68. Springer, New York.

Needleman, A. (1979). Non-normality and bifurcation in plane strain tension and compression. *J. Mech. Phys. Solids* **27**, 231–254.

Peirce, D., Asaro, R. J. and Needleman, A. (1982). An analysis of nonuniform and localized deformation in ductile single crystals. *Acta Metall.* **30**, 1087–1119.

Raniecki, B. and Bruhns, O. T. (1981). Bounds to bifurcation stresses in solids with non-associated plastic flow law at finite strains. *J. Mech. Phys. Solids* **29**, 153–172.

Rice, J. R. (1977). The localization of plastic deformation. In *Theoretical and Applied Mechanics* (Edited by W. T. Koiter), pp. 207–220. North-Holland, Amsterdam.

Rudnicki, J. W. and Rice, J. R. (1975). Conditions for the localization of deformation in pressure-sensitive dilatant materials. *J. Mech. Phys. Solids* **23**, 371–394.

Simpson, H. C. and Spector, S. J. (1987). On the positivity of the second variation in finite elasticity. *Arch. Rat. Mech.* **98**, 1–30.

Simpson, H. C. and Spector, S. J. (1989). Necessary conditions at the boundary for minimizers in finite elasticity. *Arch. Rat. Mech.* **107**, 105–125.

Steif, P. S. (1986). Bimaterial interface instabilities in plastic solids. *Int. J. Solids Structures* **22**, 195–207.

Suo, Z., Ortiz, M. and Needleman, A. (1991). Stability of solids with interfaces. *J. Mech. Phys. Solids*, in press.

Thompson, J. L. (1969). Some existence theorems for the traction boundary value problem of linearized elastostatics. *Arch. Rat. Mech. Anal.* **32**, 369–399.

Triantafyllidis, N. (1980). Bifurcation phenomena in pure bending. *J. Mech. Phys. Solids* **28**, 221–245.

van Mier, J. G. M. (1984). Strain-softening of concrete under multiaxial loading conditions. Ph.D. Dissertation, De Technische Hogeschool Eidenhoven, The Netherlands.

Vardoulakis, I. and Graf, B. (1985). Calibration of constitutive models for granular materials using data from biaxial experiments. *Géotechnique* **35**, 299–317.

Waversik, W. R. and Brace, W. F. (1971). Post-failure behavior of a granite and a diabase. *Rock Mech.* **3**, 61–85.

Young, N. J. B. (1976). Bifurcation phenomena in the plane compression test. *J. Mech. Phys. Solids* **24**, 77–91.

Zbib, H. M. and Aifantis, E. C. (1988). On the localization and post-localization behavior plastic deformation. I. On the initiation of shear bands. *Res. Mech.* **23**, 261–277.